Jennifer Ziello, Shuling Zhang, Sarah Klein, Tyler Levy, Derek Papalegis, Lily Vu, Gabriella Spang, Arvin Ruiz and Giorgio Inghirami
Cell Signaling Technology, Inc., Danvers MA 01923
Abstract #6112

Spatial analysis of the DLBCL tumor microenvironment via the novel SignalStar® multiplex immunohistochemistry assay

INTRODUCTION

Diffuse Large B-Cell Lymphoma (DLBCL) is the most common type of non-Hodgkin lymphoma, accounting for more than 18,000 cases each year within the United States. While roughly 60% of patients with DLBCL achieve durable remissions with existing chemotherapies, the prognosis of patients with refractory DLBCL is poor. The immune landscape of DLBCL is complex and further elucidation of the interplay between T cell activation and immunosuppression within the tumor microenvironment (TME) is necessary in order to better stratify patients and predict outcomes for therapy. This complexity, as well as the relevance of the spatial context of the various cell types within the TME necessitate the ability to simultaneously visualize biomarkers and phenotypic markers via multiplex immunohistochemical (mIHC) assays.

METHODS

Here, we construct a 12-plex SignalStar mIHC panel consisting of T cell phenotypic, activation and suppression markers in order to characterize the TME of FFPE DLBCL cores. We visualize immuno-oncology markers in the context of the tumor and myeloid cells, as defined by CD68. In this assay, all 12 antibodies are applied in one primary incubation, followed by the addition of a network of fluorescently-labeled oligonucleotides used to amplify the signal of 4 antibody-oligo conjugates across 3 rounds of imaging. Following amplification and imaging of the first 4 conjugates, the fluorescent signal was enzymatically removed and the process repeated for two more rounds. The three resulting images were then aligned using Visiopharm's Tissuealign™ platform. Quantitative analysis, including positive cell counts and marker co-localization, was conducted with Visiopharm's Phenoplex™. Biomarker expression patterns were also examined using Phenoplex™. Finally, we correlated these data with patient demographics, disease progression, and treatment responses.

RESULTS

SignalStar mIHC staining displayed strong, specific signal in all four channels and in all three imaging rounds. Over 900 distinct phenotypes were detected upon analysis, each comprised of various combinations of the markers stained as well as a negative cell population, which did not stain for any target present in this panel. When these results were quantified, CD3+ T cells were significantly more present in the complete responders vs. the progressive disease, with a p-value of 0.018 when a Type 3 T-Test was performed. There was also substantially more PD-L1 (41% average positivity in responders vs. 16% in progressors) present in the complete responders vs. the progressive disease patients. This latter finding is discordant with what has been previously published and could potentially be an artifact of the small sample size. While there were 8 complete responders, there were only 3 disease progressors.
Furthermore, there were many clusters of complex phenotypes that were differentially present in the tissue of the complete responders vs. that of the disease progressors and vice versa. T-sne plots revealed CD68+ PD-L1+ PD-1+ TIM-3+ to be among these clusters, while a volcano plot revealed statistically significant (p-value ≤ 0.05) phenotypes such as CD3+ CD8+ LAG3+ TIM-3+ that were likewise present more so in the responders. Other statistically significant differential phenotypes, such as CD3+ PD-L1+ TIM-3+ cells, are not typically observed and may be artifacts of the extremely densely packed TME of these lymph node structures that present a challenge to accurately segment.

CONCLUSIONS

Ultimately, we demonstrate that SignalStar mIHC is a useful tool in the characterization and analysis of the complex TME. Furthermore, upon analysis, several phenotypes were found to be significantly more present in complete responders vs. disease progressors. As this study consisted of a small sample size, we hope to expand on this dataset in order to confirm these findings. Many of these clusters expressed multiple immunosuppressive proteins and markers of T cell exhaustion. As our understanding of the spectrum of immune cell exhaustion and activation expands, the ability to fully characterize the incredibly diverse phenotypes of T cells within and surrounding the tumor is crucial in order to better predict outcome. The ability of staining and analysis such as that performed in this study empowers researchers to more effectively stratify patients, potentially improving treatment response and outcome.

Figure 1: How SignalStar mIHC Works

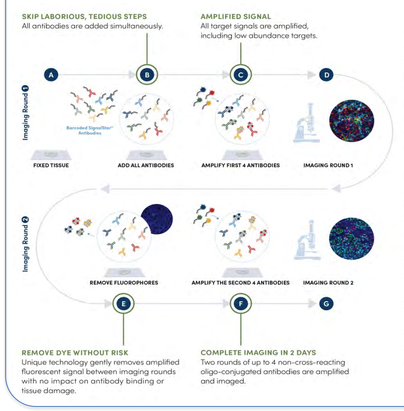

Figure 1. The SignalStar assay allows for the simultaneous labeling of up to 8 targets in formalin-fixed paraffin embedded (FFPE) tissue. Deparaffinized and rehydrated FFPE tissue sections undergo antigen retrieval (A), and all antibodies in your plex-size of choice (3-8 maximum unique oligo-conjugated antibodies) are added in one primary incubation step (B). A network of complementary oligos with fluorescent dyes (excitations: 488, 594, 647, 750) amplify the signal of up to 4 antibodies in the first round of imaging (C-D). If the plex-size is greater than 4, the first round of oligonucleotides and fluorophores are gently and specifically removed (E), and a second round of amplification is performed to visualize up to 4 additional oligo-conjugated antibodies (F). The two images are then aligned and fused computationally with either proprietary or open-source software to generate the full up to 8-plex image (G).

Figure 2: 12-plex SignalStar mIHC Panel

A.

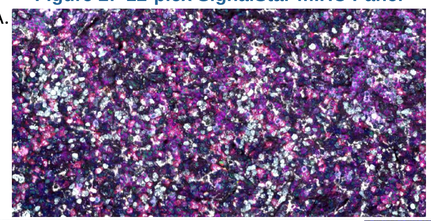

B.

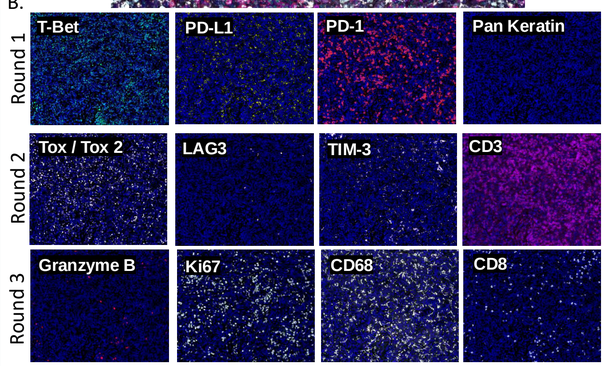

C.

Primary Antibody Marker (clone)	Imaging Round	Fluor	Psuedocolor
T-bet/TBX21 (E4I2K)	1	488	Green
PD-L1 (E1L3N®)	1	594	Yellow
PD-1 (Intracellular Domain) (D4W2J)	1	647	Red
Pan-Keratin (C11)	1	750	Cyan
Tox/Tox2 (E6I3Q)	2	488	Pink
LAG3 (D2G40™)	2	594	Orange
TIM-3 (D5D5R™)	2	647	Periwinkle
CD3ε (D7A6E™)	2	750	Magenta
Granzyme B (D6E9W)	3	488	Burgundy
Ki-67 (8D5)	3	594	White
CD68 (D4B9C)	3	647	Light Pink
CD8α (D8A8Y)	3	750	Purple

Figure 2A. SignalStar 12-plex multiplex immunohistochemical staining of formalin fixed, paraffin-embedded human DLBCL tissue. **Figure 2B**. Breakdown into the individual channels of SignalStar multiplex staining showed in Figure 2A. **Figure 3C.** The composition of the SignalStar multiplex panel used to stain the image in Figure 2A.

Figure 3: % Positivity of each Target in Complete Responders vs. Progressors

A.

	Core 1C	Core 1D	Core 2D	Core 2A	Core 3C	Core 3F	Core 5B	Core 5E	Core 4E	Core 2F	Core 5F
Ki-67	57%	87%	91%	73%	44%	71%	10%	60%	83%	49%	66%
CD3	23%	0%	2%	39%	49%	21%	20%	30%	7%	5%	3%
Tox/Tox2	49%	70%	1%	38%	84%	91%	17%	93%	89%	37%	17%
PD-1	28%	36%	20%	5%	36%	7%	41%	48%	9%	84%	23%
LAG3	13%	1%	13%	95%	13%	7%	10%	16%	7%	0%	7%
CD68	14%	13%	13%	8%	18%	11%	5%	9%	13%	5%	9%
PDL1	45%	7%	66%	43%	55%	9%	55%	48%	22%	2%	24%
TIM-3	73%	13%	90%	25%	98%	52%	95%	98%	44%	90%	94%
Granzyme B	3%	0%	0%	15%	11%	7%	8%	13%	10%	2%	1%
CD8	5%	1%	1%	21%	57%	14%	13%	25%	7%	3%	20%
Negative	9%	5%	1%	2%	1%	1%	4%	1%	4%	1%	2%

Complete Response | Progressive Disease

B.

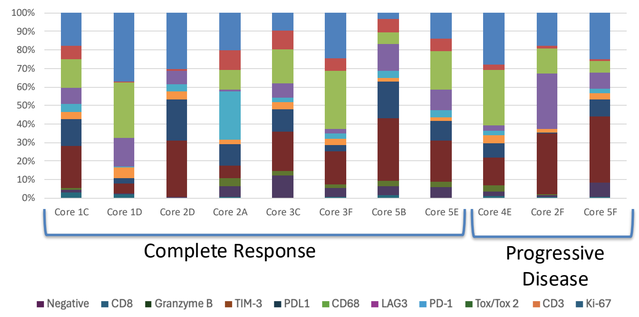

C.

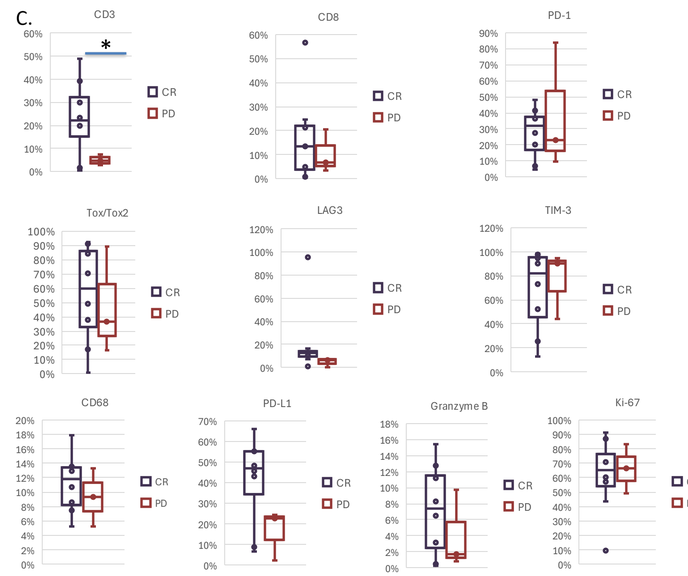

Figure 3A. Heat map of the percentages of each target present in each core with red denoting more expression and blue lower expression. Cores are grouped according to final response to therapy. **Figure 3B.** Component bar chart of the distribution of each target present in each core. **Figure 3C**. Box plots of the percentage of each target present in each core. Statistical significance denoted by asterisk and set at p=0.05 and performed with a 2-tailed Students t-Test assuming unequal variances.

Figure 4: Differential Phenotypes Present in Complete Responders vs. Progressors

A.

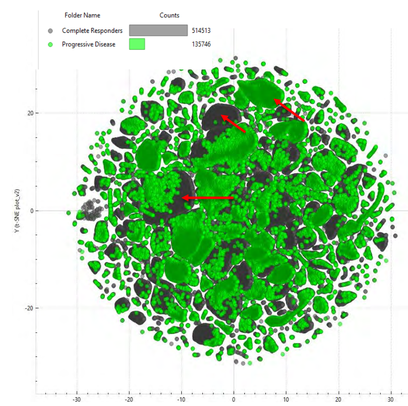

B.

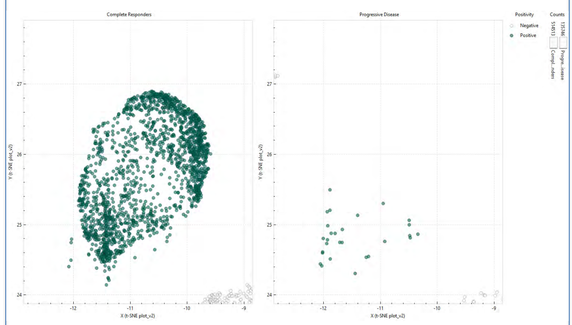

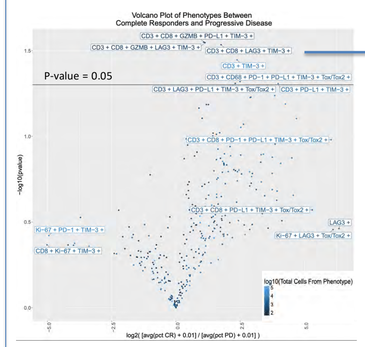

D.

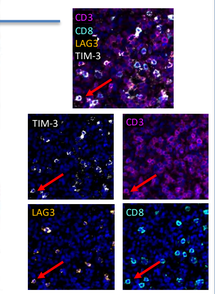

Figure 4A. DLBCL FFPE tissue was stained with the SignalStar panel shown in Figure 1C and subsequently analyzed with the Viospharm Phenoplex software. A T-sne plot is shown with all phenotypes present in complete responders (grey) and disease progressors (green). Various clusters of phenotypes that are present in the complete responders vs. the progressors and vice versa can be observed (red arrows). **Figure 4B**. An example of a cluster of CD68+PD-L1+PD-1+TIM-3+ present in the complete responders but absent in those with progressive disease. **Figure 4C.** A volcano plot of the phenotypes that were found to be differentially expressed in the complete responders (shown on the right) vs. the progressors (shown on the left). Each dot represents a distinct phenotype while the color indicates the number of cells which express that phenotype. P value is shown on the y-axis while fold change is shown on the x-axis. The p-value of 0.05 is denoted by the black horizontal line. Several of the phenotypes with the highest fold change and p-value are labelled. **Figure 4D**. Representative images showing one of the phenotypes present at an increased frequency in the complete responders. A CD3+ (magenta) CD8+ (cyan) LAG3+ (orange) TIM-3+ (white) cell is denoted by the red arrows.

Jennifer Ziello
email: Jennifer.Ziello@cellsignal.com
cellsignal.com/posters